dence to date that individual neurons have the capacity to generate circadian rhythms. Cultured hypothalamic neurons of mammals show a circadian rhythm in the release of vasopressin (9), but the rhythm was measured after sufficient time for functional connections to be restored. Thus it is not yet certain whether individual hypothalamic neurons have the capacity to generate circadian rhythms.

Although we have demonstrated that individual neurons can generate a circadian rhythm, it is not clear whether isolated neurons have all of the characteristics associated with the "biological clock" in the intact retina (for example, entrainment by Zeitgebers, temperature compensation). Indeed, we failed to observe light responses from BRNs in culture, even though BRNs in the intact retina depolarize upon illumination and can be phase-shifted (*10*). In addition, we only rarely observed impulse production in dispersed cells. Regardless of whether some properties of circadian systems require organized tissue, our experiments confirm that the mechanisms for generation and expression of circadian rhythmicity can be present within individual neurons. This demonstration should greatly aid experimental efforts to understand the cellular basis of circadian rhythm generation by facilitating the use of biophysical and biochemical techniques with identified circadian pacemaker cells.

REFERENCES AND NOTES

1. F. Turek, *Annu. Rev. Physiol.* **47**, 49 (1985); J. Takahashi, N. Murakami, S. S. Nikaido, B. L. Pratt, L. M. Robertson, *Recent Progr. Horm. Res.* **45**, 279 (1989); J. W. Jacklet, in *Neuronal and Cellular Oscillators*, J. W. Jacklet, Ed. (Dekker, New York, 1989), pp. 483–527.
2. T. Deguchi, *Nature* **282**, 94 (1979); L. M. Robertson and J. S. Takahashi, *J. Neurosci.* **8**, 12 (1988); M. Zatz, D. A. Mullen, J. R. Moskal, *Brain Res.* **438**, 199 (1988).
3. J. W. Jacklet, *Science* **164**, 562 (1969); A. Eskin, *Fed. Proc. Fed. Am. Soc. Exp. Biol.* **38**, 2573 (1979); _____ and E. Harcombe, *Comp. Biochem. Physiol. A* **57**, 443 (1977); G. D. Block and M. H. Roberts, *J. Comp. Physiol. A* **142**, 403 (1981).
4. G. D. Block and S. F. Wallace, *Science* **217**, 155 (1982); G. D. Block and D. G. McMahon, *J. Comp. Physiol. A* **155**, 387 (1984).
5. D. G. McMahon, S. F. Wallace, G. D. Block, *J. Comp. Physiol. A* **155**, 379 (1984).
6. D. G. McMahon, thesis, University of Virginia (1986); M. R. Ralph and G. D. Block, *J. Comp. Physiol. A* **166**, 589 (1990). Previous conductance measurements were made between Zeitgeber time (ZT) 19 and 6 or between 10 and 17. The only observed transitions were at projected dawn or dusk. Zeitgeber time refers to the time during a 24-hour cycle in which ZT 0 equals projected dawn, the hour at which the light onset would have occurred if the animals had remained on the light-dark cycle.
7. D. G. McMahon and G. D. Block, *J. Comp. Physiol. A* **161**, 335 (1987). The recording dish was continuously perfused with artificial seawater (ASW). Thin-wall glass electrodes (20 to 40 megohms) were used.
8. S. B. Khalsa, M. R. Ralph, G. D. Block, *Soc. Neurosci. Abstr.* **17**, 1240 (1991).
9. N. Murakami *et al.*, *Brain Res.* **545**, 347 (1991).
10. G. D. Block and D. G. McMahon, *ibid.* **265**, 134 (1983); M. E. Geusz and T. L. Page, *J. Comp. Physiol. A* **168**, 565 (1991).
11. Leibovitz L-15 medium (Sigma, ICN) was modified according to the procedure of S. Schacher and E. Proshansky [*J. Neurosci.* **3**, 2403 (1983)], with hemolymph omitted and gentamicin added (0.1 mg/ml, Sigma). Osmolarity was corrected to that of ASW, and pH was 7.4 to 7.8. Intact eyes maintained in the medium showed circadian rhythms with normal period and phase.
12. The criteria consisted of a cell diameter less than 50 μm, the presence of large organelle-like structures not found in the photoreceptors, and the lack of pigment granules associated with cells of the distal retina [J. W. Jacklet and W. Colquhoun, *J. Neurocytol.* **12**, 673 (1983)]. The large inclusions characteristic of BRNs are evident after dye-fills of cells identified positively as BRNs in eye preparations [M. E. Geusz and G. D. Block, *J. Biol. Rhythms* **7**, 255 (1992)].
13. Criteria for stability consisted of a resting potential between −25 and −65 mV, no more than 5-mV drift between first and last current pulses, and no regions of negative slope of the current-voltage curves. Cells that did not show at least a 5-mV change in membrane potential due to an injected current of −0.2 nA were rejected as having poor membrane sealing. We attempted recordings from 290 cells from 114 retinae. Of these, 32 cells yielded stable membrane potential records with balanced electrodes about 1 min after impalement. Many cells lysed upon impalement.
14. A *t* value was used to determine the significance of the effect of group (before dawn or after dawn) in a multiple linear regression model with SPSS/PC+ (SPSS Inc.), with the change in membrane potential as the dependent variable and current and group as independent variables.
15. Criteria for stability used for isolated cells were the same as for cells dispersed on cover slips. We attempted recordings from 155 cells from 172 retinae. Of these, 55 cells yielded stable membrane potential records.

16. We thank F. Strumwasser, B. Kellams, S. Schacher, S. Dryer, and L. Latham for instruction or assistance with cell culture techniques and W. O. Friesen and T. Page for reviewing an early version of the manuscript. Supported by NIH grant NS15264 to G.D.B. S.M. was supported by the Deutsche Forschungsgemeinschaft and the NSF Center for Biological Timing; M.E.G. received support from NIH grant NS08806; and J.J.Z. was supported by the Undergraduate Research Program of the NSF Center for Biological Timing.

23 September 1992; accepted 13 November 1992

Tyrosine Phosphorylation of Actin in *Dictyostelium* Associated with Cell-Shape Changes

Peter K. Howard, Bartholomew M. Sefton, Richard A. Firtel*

When *Dictyostelium* cells that have initiated their developmental program upon starvation are returned to growth medium, there is a rapid and transient de novo tyrosine phosphorylation of a 43-kilodalton protein. This protein was found to be actin. Most of the phosphorylation occurred in a single, minor acidic isoform of actin. Developing cells that had been returned to growth medium lost their pseudopod extensions, became round, and had reduced adhesion to the substratum. These effects occurred with kinetics that matched the increase in tyrosine phosphorylation of actin. In mutant cell lines in which the gene for the phosphotyrosine phosphatase PTP1 had been disrupted, tyrosine phosphorylation of actin was rapid and more prolonged. These cells responded with proportionally accelerated kinetics of cell rounding. Cell lines overexpressing PTP1 had diminished amplitude and duration of actin tyrosine phosphorylation and exhibited diminished cell-shape change and an accelerated return to the extended cell-shape morphology seen in starved cells.

A variety of extracellular signals, such as growth factors and chemoattractants, and intrinsic events, such as progression through the cell cycle, lead to changes in cell shape and altered filamentous (F)-actin (*1*). Changes in actin and the cytoskeleton occur in *Dictyostelium* after stimulation of cells by the chemoattractant adenosine 3′,5′-monophosphate (cAMP) (*2*). Binding of cAMP to surface receptors leads to polymerization of actin within seconds and subsequent changes in the association of actin binding proteins with actin and the cytoskeleton. These responses lead to specific morphological changes within the cell and to extension of pseudopodia in the direction of the emitted cAMP signal. Little is known, however, about the signal transduction steps that connect the initial signaling events to the morphological changes. Changes in the Ca^{2+} concentration are thought to regulate some actin binding protein associations with the cytoskeleton (*3*), and in *Dictyostelium* the 1,2-diacylglycerol stimulates actin polymerization by apparent de novo formation of actin nucleation sites (*4*). We provide evidence that changes in the tyrosine phosphorylation of actin correlate with changes in the cell shape in *Dictyostelium*.

Changes in protein tyrosine phosphorylation have been examined through the *Dictyostelium* developmental cycle by protein immunoblotting with antibodies to

P. K. Howard and R. A. Firtel, Department of Biology, Center for Molecular Genetics, University of California, San Diego, La Jolla, CA 92093.
B. M. Sefton, Molecular Biology and Virology Laboratory, The Salk Institute for Biological Sciences, San Diego, CA 92186.

*To whom correspondence should be addressed.

phosphotyrosine (anti-pTyr) (5). A 43-kD protein is weakly labeled by the anti-pTyr in vegetative cells (Fig. 1) and is no longer labeled in cells 1 hour after the cells have initiated development (5). Cells were starved in suspension culture in nonnutrient buffer for 4 hours to initiate early developmental gene expression and then returned to standard *Dictyostelium* axenic growth medium (HL5) (6). At 5-min intervals after return to growth medium, proteins from cells were analyzed by protein immunoblotting with anti-pTyr. Phosphorylation of a 43-kD protein increased substantially relative to the amount of phosphorylation of that protein in cells that had been starved for 4 hours or to the steady-state amount of phosphorylation in vegetatively growing cells (Fig. 1). Tyrosine phosphorylation of p43 was detectable within 5 min and was maximal by 20 min, when it was the most prominent pTyr-containing protein. The intensity of the signal then decreased gradually to a faint but detectable signal after several hours (7). When developing cells that had been returned to growth medium for 20 min (henceforth referred to as growth-stimulated cells) were starved in salts without nutrients (8), the pTyr signal on p43 rapidly decreased and was not detectable within 25 min (Fig. 1).

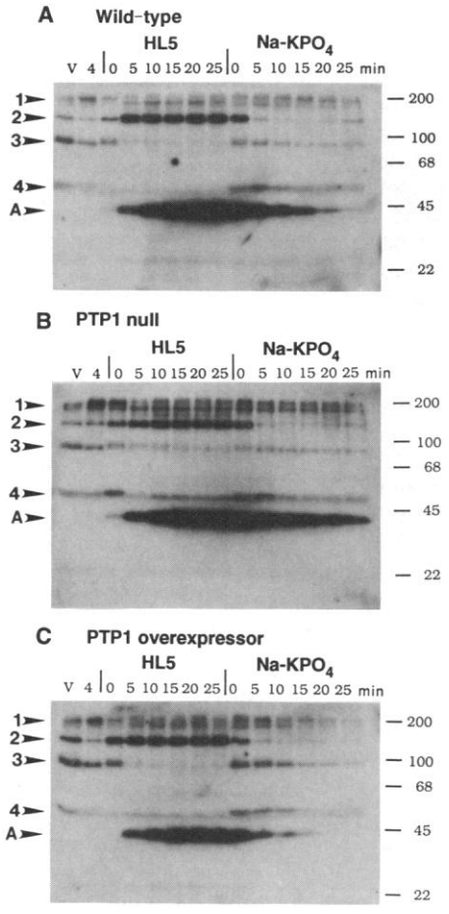

Shifts from starvation conditions to growth medium and then back to starvation conditions resulted in changes in the amount of tyrosine phosphorylation of at least four other proteins (Fig. 1). Increased phosphorylation of the ~130- and 55-kD phosphoproteins was the earliest detectable change after stimulation of cells with growth medium, whereas the dephosphorylation of a 90-kD protein was the first change detected after return to starvation.

PTP1 is a developmentally regulated tyrosine phosphatase in *Dictyostelium* and is required for the normal temporal pattern of development. PTP1 is expressed in low amounts during vegetative growth, and its expression is spatially regulated during multicellular development (5). We examined whether PTP1 might participate in the phosphorylation-dephosphorylation cycle of pp43 by repeating the nutrient-shift experiments with *ptp1* null cells carrying a disrupted *PTP1* gene and with cell lines overexpressing PTP1 (5). In PTP1-overexpressing mutants, the amount of tyrosine phosphorylation of p43 upon the return of cells to growth medium was one-third to one-fourth of that in wild-type cells, and the rate of dephosphorylation was 10 to 20 times more rapid when cells were returned to nonnutrient buffer (Fig. 1). In *ptp1* null strains, although the extent of tyrosine phosphorylation of p43 was similar to that in wild-type cells, the maximum amount of phosphorylation was attained in 10 to 15 min versus 20 to 25 min, and the rate of dephosphorylation of p43 was one-fifth of that in wild-type cells, with much of the phosphorylation remaining 30 min after cells were returned to nonnutrient buffer. The amount of PTP1 had little effect on the phosphorylation of the other prominent phosphoproteins, with the exception of p90, which showed little change in the amount of tyrosine phosphorylation in *ptp1* null cells.

The protein p43 comigrates with actin on polyacrylamide gels (7). We immunoprecipitated actin from a lysate of growth-stimulated cells with an antibody to actin (anti-actin) (9) and found that the precipitated protein reacted with anti-pTyr (7). This suggested that p43

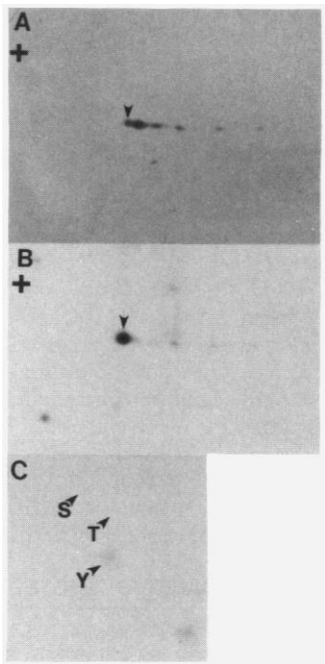

Fig. 1. Changes in protein tyrosine phosphorylation in response to nutrient shift in (**A**) wild-type cells, (**B**) PTP1 null cells, and (**C**) PTP1 overexpressor cells. Logarithmically growing vegetative wild-type cells (axenic strain KAx-3) were harvested, washed, and suspended in sodium and potassium phosphate salts not buffered by the nutrients (8) to initiate development and shaken at 180 rpm. After 4 hours, cells were centrifuged and resuspended in HL5 growth medium (8). Cells were collected every 5 min and boiled in SDS sample buffer. After 25 min, the remaining cells were washed free of nutrients, resuspended in salts not buffered by the nutrients, and sampled every 5 min as described. Proteins were resolved by SDS–polyacrylamide gel electrophoresis (PAGE) on 10% gels, blotted, and probed with anti-pTyr and ^{125}I-labeled protein A as described (19). Molecular size markers are shown at the right (in kilodaltons). V, vegetative cells; 4, cells starved for 4 hours. HL5, time points of cells resuspended in HL5; Na-KPO$_4$, time points of cells resuspended in buffer. Arrowheads mark proteins that undergo tyrosine phosphorylation: 1, protein >200 kD; 2, p130; 3, p90; 4, p55; A, actin. Rates of tyrosine phosphorylation and dephosphorylation were quantitated with a Phosphoimage analyzer.

Fig. 2. Tyrosine phosphorylation of actin in response to nutrient shift. KAx-3 cells were grown in suspension for 12 hours in MES-buffered HL5 to 2 × 10^6 to 5 × 10^6 cells per milliliter, washed free of medium, and resuspended at 1 × 10^7 cells per milliliter in medium not buffered by phosphates or containing nutrients (MES-PDF) (8). Five millicuries of ^{32}PO$_4$ were added, and cells were starved in suspension culture for 4 hours. An equal volume of 2× MES-FM medium [a defined, axenic growth medium that does not contain phosphates (14)] was added, and cells were shaken for an additional 30 min. Cells pelleted by centrifugation were boiled in SDS lysis buffer and immunoprecipitated with affinity-purified polyclonal rabbit antibodies to actin (9). The affinity-purified proteins were fractionated by two-dimensional PAGE [LKB ampholytes, pH range of 3.5 to 10 (10)], transferred to an Immobilon membrane, stained with the anti-actin, and visualized with a colorimetric detection system (**A**) (more acidic proteins on the left) or by autoradiography (**B**). The portion of the gel containing actin (10) is shown. The major ^{32}P-labeled spot was excised and subjected to a two-dimensional phosphoamino acid analysis as described (20) (**C**). The positions of phosphoserine (S), phosphothreonine (T), and phosphotyrosine (Y) are indicated.

was actin. To show that actin undergoes tyrosine phosphorylation, we partially purified actin from cells labeled biosynthetically with [^{32}P]orthophosphate. Actin was immunoprecipitated from growth-stimulated cell lysates with the anti-actin. The immunoprecipitated proteins were fractionated by two-dimensional polyacrylamide gel electrophoresis (*10*), transferred to an Immobilon-P membrane, and stained with anti-actin and alkaline phosphorylase–coupled second antibody. The ^{32}P-labeled proteins were detected by autoradiography. Most of the radioactivity was associated with the most acidic isoform, which we estimate represents 10 to 15% of the total actin (Fig. 2B). When this labeled spot was excised and subjected to phosphoamino acid analysis, phosphotyrosine was detected (Fig. 2C). In *Dictyostelium*, ~20 distinct actin genes have been identified (*11*). Of the ones that have been analyzed, most have identical amino acid sequences, although some isoforms have been identified by sequence analysis and two-dimensional gel analysis (*10*). We do not know whether the phosphorylation occurs on a minor species or whether the phosphorylated isoform is generated by tyrosine phosphorylation of a major actin isoform.

Cells transferred from starvation conditions to growth medium showed a transient change in cell shape. We examined the kinetics of tyrosine phosphorylation of actin, changes in plasma membrane–associated F-actin, and cell shape in wild-type and PTP1 mutant cell lines responding to the addition of growth medium. Cells were starved in suspension (which also initiates development) for 4 hours and allowed to settle on glass cover slips; the starvation buffer was then replaced either with fresh starvation buffer (as a control) or with growth medium. At chosen time points, cells were fixed and stained with rhodamine-labeled phalloidin to detect F-actin–containing structures (*12*). Wild-type cells plated onto cover slips in nonnutrient buffer became well spread and adherent, with spike-like projections of F-actin at the plasma membrane (Fig. 3, A and D). By 10 min after the addition of growth medium, the cells became round, and F-actin–containing cellular projections, although numerous, became quite short (Fig. 3, B and E); ~50% of the cells no longer adhered to the cover slip. After 20 min, 95% of the cells no longer adhered to the surface, and the few remaining cells were still round (Fig. 3, C and F). In comparison, in wild-type or PTP1 mutant cells exposed to nonnutrient buffer, there was no change in the amount of actin tyrosine phosphorylation or in the cell shape. The *ptp1* null cells plated in starvation buffer were also adherent and exhibited F-actin projections, although these projections were less numerous than in wild-type cells (Fig. 3G). By 10 min after replacement of the buffer with growth medium, these cells had become quite round, and 95% had become detached from the cover slip (Fig. 3H), similar to that observed for wild-type cells after 20 min. The morphology and number of cells attached to the cover slip were unchanged after 20 min (Fig. 3I). PTP1-overexpressing cells that had been starved for 4 hours spread out on the cover slip and contained more numerous spike-like F-actin projections than wild-type cells (Fig. 3J). After 10 min in growth medium, these cells started to become round; however, many cells retained F-actin projections, and by 20 min these cells had begun to spread and re-extend F-actin–containing structures and had attained a cell shape similar to that of starved cells (Fig. 3, K and L). In contrast to wild-type and *ptp1* null cells, there was little loss of PTP1-overexpressing cells from the cover slip. Thus, in PTP1-overexpressing cells, the cell-shape change, as with the actin tyrosine phosphorylation, was transient, whereas in the *ptp1* null cells the extent of actin phosphorylation and the rate of cell-shape change were more rapid. When cells that had been starved for 4 hours were initially plated on a glass surface and subjected to the same changes in medium, we observed similar kinetics of both actin tyrosine phosphorylation and cell-shape change to those seen when cells in suspension were used (*7*).

Amino acid starvation initiates the developmental phase of the *Dictyostelium* life cycle (*13*). When starved cells were returned to a chemically defined minimal medium (*14*), actin tyrosine phosphorylation and cell-shape changes occurred as with cells that had been returned to growth medium (*7*). We determined which components of the defined medium elicit the response by adding various components to cells starved for 4 hours in nonnutrient buffer. Both amino acids and glucose were necessary and sufficient to induce actin tyrosine phosphorylation with the same kinetics as growth medium.

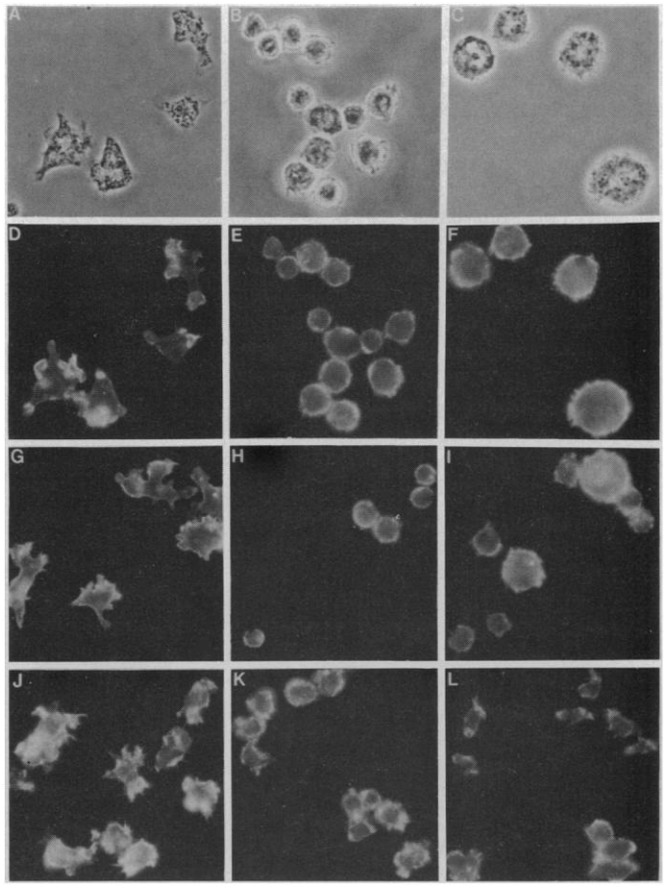

Fig. 3. Cell-shape changes in response to return to growth conditions. Cells were grown, harvested, and starved as described (Fig. 1). After 3.5 hours, the cells were plated onto cover slips and allowed to settle for 0.5 hour. The medium was then exchanged with either buffered salts or HL5 growth medium. For immunofluorescence of F-actin, cells were fixed as described (*12*), stained with rhodamine-phalloidin (Molecular Probes, Inc., 3.3 μM in buffer) (*12*) for 20 min in the dark, and rinsed in the same buffer with 0.05% Tween. (**A** to **C**) Phase-contrast photomicrographs of wild-type cells at 4 hours starvation (A), after 10 min in HL5 (B), and after 20 min in HL5 (C). (**D** to **F**) Rhodomine-phalloidin fluorescence of the same cells shown in (A) (D), (B) (E), and (C) (F), respectively. (**G** to **I**) Rhodomine-phalloidin fluorescence of the *ptp1* null mutant cells at 4 hours after starvation (G), after 10 min in HL5 (H), and after 20 min in HL5 (I). (**J** to **L**) Fluorescence photographs of the PTP1-overexpressing cells stained with rhodomine-phalloidin at 4 hours after starvation (J), after 10 min in HL5 (K), and after 20 min in HL5 (L). Selected regions of the field are presented to show representative cell shapes and to indicate relative adherence to the cover slips. Quantitation of numbers of cells adhering was performed by cell count in a 20-mm^2 field. All photomicrographs are the same magnification.

Our results show a temporal correlation between tyrosine phosphorylation of actin and cell-shape changes in response to growth conditions and suggest that growth medium induces either the activation of a tyrosine kinase or inhibition of a phosphotyrosine phosphatase that regulates actin tyrosine phosphorylation. This phosphorylation may in turn regulate the alterations in F-actin–containing structures in the cytoskeleton, resulting in cell-shape changes. Changes in the amount of PTP1 affect the kinetics and extent of actin phosphorylation and similarly affect the kinetics and extent of the cell-shape changes and F-actin staining pattern. It is possible that PTP1 does not directly dephosphorylate pTyr-actin and that the effects of PTP1 activity may be propagated through a series of responding proteins. Because the amount of growth-stimulated actin tyrosine phosphorylation in *ptp1* null cells decreases to an amount similar to that seen in wild-type cells, a second PTP may dephosphorylate actin in the absence of PTP1. *Amoeba proteus* actin is phosphorylated in vitro in cell-free extracts in response to Ca^{2+} (the phosphorylated amino acid is unknown) and has been shown to affect actin polymerization in vitro (*15*). Although actin phosphorylation has not been reported in vertebrates, tyrosine phosphorylation of nonactin proteins is essential for conversion of globular (G)-actin to F-actin in B lymphocytes (*16*). The observed changes in *Dictyostelium* may be analogous to cytoskeleton changes in mammalian cells mediated by serum and other extracellular factors or protooncogene activation (*17*).

Note added in proof. Schweiger *et al.* (*18*) also recently showed pTyr-actin in *Dictyostelium*.

REFERENCES AND NOTES

1. S. R. Farmer and L. E. Dike, in *Cell Shape Determinants, Regulatory Role*, W. D. Stein and F. Bronner, Eds. (Academic Press, San Diego, CA, 1989), pp. 173–202; W. Kabsch and J. Vandekerckhove, *Annu. Rev. Biophys. Biomol. Struct.* **21**, 49 (1992).
2. G. Gerisch, *Annu. Rev. Physiol.* **44**, 535 (1982); S. J. McRobbie and P. C. Newell, *Biochem. Biophys. Res. Commun.* **115**, 351 (1983); S. J. McRobbie, *CRC Crit. Rev. Microbiol.* **13**, 335 (1986); P. N. Devreotes and S. H. Zigmond, *Annu. Rev. Cell Biol.* **4**, 649 (1988); J. Condeelis, *Dev. Genet.* **11**, 333 (1990); C. H. Berlot, J. A. Spudich, P. N. Devreotes, *Cell* **43**, 307 (1985); S. Yumura and Y. Fukui, *Nature* **314**, 194 (1985); R. P. Futrelle, J. Traut, W. George McKee, *J. Cell Biol.* **92**, 807 (1982).
3. A. Weeds, *Nature* **296**, 811 (1982); T. D. Pollard and J. A. Cooper, *Annu. Rev. Biochem.* **55**, 987 (1986).
4. A. Shariff and E. J. Luna, *Science* **256**, 245 (1992).
5. P. Howard, B. Sefton, R. A. Firtel, *Cell* **71**, 637 (1992).
6. HL5 contains yeast extract, peptone, glucose, and salts.
7. P. Howard, B. Sefton, R. A. Firtel, unpublished data.
8. M. Mehdy and R. A. Firtel, *Mol. Cell. Biol.* **5**, 705 (1985).
9. Cells were lysed in 0.5% SDS, 1 mM dithiothreitol, and 50 mM tris (pH 8.8) and then diluted with 4 volumes of RIPA buffer without SDS [0.15 M NaCl, 0.01 M $NaPO_4$ (pH 7.2), 1% aprotinin, 1% sodium deoxycholate, 1% NP-40]. Lysates were incubated with antibody for 40 min at 4°C and then with protein A–conjugated Sepharose beads for 40 min. After centrifugation, the sedimental beads were rinsed four times with RIPA buffer.
10. J. I. Garrels and W. Gibson, *Cell* **9**, 793 (1976); C. MacLeod, R. A. Firtel, J. Papkoff, *Dev. Biol.* **76**, 263 (1980); P. Romans and R. A. Firtel, *J. Mol. Biol.* **186**, 337 (1985).
11. M. McKeown and R. A. Firtel, *J. Mol. Biol.* **151**, 593 (1981); *Cold Spring Harbor Symp. Quant. Biol.* **46**, 495 (1982).
12. P. A. Amato, E. R. Unanue, D. L. Taylor, *J. Cell Biol.* **96**, 750 (1983); A. L. Hall, A. Schlein, J. Condeelis, *J. Cell. Biochem.* **37**, 285 (1988).
13. F. T. Marin, *Dev. Biol.* **48**, 110 (1976).
14. J. Franke and R. Kessin, *Proc. Natl. Acad. Sci. U.S.A.* **74**, 2157 (1977).
15. J. Sonobe, S. Takahashi, S. Hatano, K. Kuroda, *J. Biol. Chem.* **261**, 14837 (1986).
16. I. Melamed, G. P. Downey, C. M. Roifman, *Biochem. Biophys. Res. Commun.* **176**, 1424 (1991).
17. V. Ambros, L. B. Chen, M. Buchanan, *Proc. Natl. Acad. Sci. U.S.A.* **72**, 3144 (1975); K. Mellstrom, C.-H. Heldin, B. Westermark, *Exp. Cell Res.* **177**, 347 (1988); K. Burridge, *Cancer Rev.* **4**, 18 (1986); R. G. Watts, M. A. Chrispens, T. H. Howard, *Cytoskeleton* **19**, 159 (1991).
18. A. Schweiger *et al.*, *J. Cell Sci.* **122**, 601 (1992).
19. M. P. Kamps and B. M. Sefton, *Oncogene* **2**, 305 (1988).
20. M. P. Kamps, *Methods Enzymol.* **201**, 21 (1991).
21. Anti-actin was a gift of Dr. Annamma Spudich, Stanford University [P. A. Simpson, J. A. Spudich, P. Parham, *J. Cell Biol.* **99**, 287 (1984)]. We thank members of the laboratories of R. A. Firtel, B. Sefton, and T. Hunter and R. Gomer for helpful suggestions. Supported by U.S. Public Health Service grants to R.A.F. and B.S.

17 August 1992; accepted 16 October 1992

Forward Plasma Membrane Flow in Growing Nerve Processes

Sergey Popov,* Abraham Brown, Mu-ming Poo†

Nerve growth requires addition of new plasma membrane material, which is generally believed to occur at the growth cone. Local incorporation of a fluorescent lipid analog into the plasma membrane of fast-growing *Xenopus* neurites revealed an anterograde bulk membrane flow that correlated with neurite elongation. The rate of membrane flow depended on the position of the labeled membrane segment along the neurite, increasing with distance from the soma. This result suggests that new membrane in growing *Xenopus* neurites is added not at the growth cone but at the cell body and along the neurite.

It is generally accepted that the new plasma membrane material required for nerve growth is added at the tip of the neurite, known as the growth cone (*1*). This view of nerve growth originated mainly from the observation that extracellular particles attached to the neurite surface remain stationary relative to the soma as the neurite elongates (*2*). However, it is possible that some of the particles on the neurite surface were anchored to the neuronal cytoskeleton through transmembrane linkage, and the behavior of the particles reflects the movement of the cytoskeleton rather than that of the plasma membrane (*3*, *4*). Here we show that when fluorescent lipid molecules are locally inserted into the plasma membrane of *Xenopus laevis* neurites, they move forward as the neurite grows; thus, in this system, membrane is added not at the growth cone but at the soma and along the length of neurite.

Cultured *Xenopus* spinal neurons were prepared on laminin-coated glass cover slips (*5*) and were used 3 to 8 hours after plating. At this time, the average rate of neurite extension was 79 ± 19 μm/hour (SEM, n = 49) at room temperature (20° to 22°C). In the first set of experiments, neurons with relatively long neurites (~400 μm) were selected, and the fluorescent lipid analog 1,1′-didodecyl-3,3,3′,3′-tetramethylindocarbocyanide perchlorate ($DiIC_{12}$) was incorporated into a segment of neurite membrane close to the growth cone (at a distance of 60 to 80 μm from the neurite tip) by a local perfusion method (*6*). Analysis of the differential interference contrast (DIC) and fluorescence images of the neurite at two different times after local perfusion of the fluorescent lipid (Fig. 1) revealed that the incorporated lipid molecules rapidly spread along the membrane. The profiles of the fluorescence distribution during the first 5 min after perfusion were measured with a digital imaging method (*7*), and the positions of the center of the profiles were determined (*8*). For actively growing neurites (Fig. 1, A through C), we observed a shift of the center of the profile in the anterograde direction. In 17 cases in which elongation of the neurites was observed, the center of the fluorescence profile moved forward at a rate of 2.1 ± 0.2 μm/min (SEM) as the neurite elongated at a rate of

Department of Biological Sciences, Columbia University, New York, NY 10027.

*On leave from the Institute of Electrochemistry, Academy of Sciences, Moscow, Russia.
†To whom correspondence should be addressed.